Turbomachinery Degradation Monitoring Using Adaptive Trend Analysis ⋆

Marta Zagorowska * **Arne-Marius Ditlefsen** **
Nina F. Thornhill * **Charlotte Skourup** **

* *Department of Chemical Engineering, Imperial College London, South Kensington, SW7 2AZ London, UK (e-mail: m.zagorowska@imperial.ac.uk, n.thornhill@imperial.ac.uk)*
** *ABB Oil, Gas and Chemicals, Ole Deviks vei 10, 0666 Oslo, Norway (e-mail: arne-marius.ditlefsen@no.abb.com, charlotte.skourup@no.abb.com)*

Abstract: Performance deterioration in turbomachinery is an unwanted phenomenon that changes the behaviour of the system. It can be described by a degradation indicator based on deviations from expected values of process variables. Existing models assume that the degradation is strictly increasing with fixed convexity and that there are no additional changes during the considered operating period. This work proposes the use of an exponential trend approximation with shape adaptation and apply it in a moving window framework. The suggested method of adjustment makes it possible for the model to follow the evolution of the indicator over time. The approximation method is then applied for monitoring purposes, to predict future degradation. The influence of the tuning parameters on the accuracy of the algorithm is investigated and recommendations for the values are derived. Finally, directions for further work are proposed.

Keywords: Trends, Function approximation, Device degradation, Fault detection, Prediction methods, Compressors

1. INTRODUCTION

Turbomachinery degradation is a complex process. According to Tarabrin et al. (1996), the loss of performance is mostly due to fouling, i.e. forming the deposits on the blades and influencing the flow path. In industrial applications, degradation is measured using an indicator based on deviations from expected values of process variables (Tarabrin et al., 1996; Li and Nilkitsaranont, 2009). Monitoring of these phenomena provides an insight into the condition of the equipment, and is used, e.g., for maintenace planning (Xenos et al., 2016). The available models assume that the degradation is a monotonic function of time, and that the convexity is fixed, i.e. the geometric properties related to the graph of the function (Davidson and Donsig, 2009) are constant. For the purpose of this work, this graphic interpretation is described as the *shape* of a function. As shown by Madsen and Bakken (2014), the assumptions about the shape of the degradation indicator are not always fulfilled. This work presents a modelling approach that captures the observed behaviour of the degradation indicator. The proposed framework is then used for monitoring to predict changes of the trend of the indicator.

⋆ Financial support is gratefully acknowledged from the Marie Curie Horizon 2020 EID-ITN project "PROcess NeTwork Optimization for efficient and sustainable operation of Europe's process industries taking machinery condition and process performance into account PRONTO", Grant agreement No 675215.

The changes of the shape of the degradation indicator might have multiple origins. Maintenance activities are one of the main causes that influence the curvature (Madsen and Bakken, 2014). As the timings of the maintenance works are known, it is possible to analyse the degradation indicator in a given operating period, as described by Cicciotti (2015) or by Hanachi et al. (2017), especially for steady state operation. A similar approach was adopted by Salamat (2012), but for a wider range of operating points. Their moving window approaches assume that degradation starts immediately after the maintenance period. However, as indicated by Li and Nilkitsaranont (2009), the degradation curvature might change during the operating period, not necessarily because of the maintenance. They proposed a moving window approach where the approximating trend is switched between linear and quadratic functions of time. Nevertheless, they assumed that the monotonicity and convexity stayed the same during the operation period, and that there was only one transition moment. The approach proposed in the current work is able to capture the behaviour of the degradation by adaptation of the shape of the trend, and to adapt to the unknown timings of the transitions.

The remainder of the paper is structured as follows. The degradation of centrifugal compressors is introduced, including a description of degradation models and their approximation. Section 3 describes the trend approximation with moving window and shape adaptation. The algorithm is then applied to prediction and evaluated for monitoring

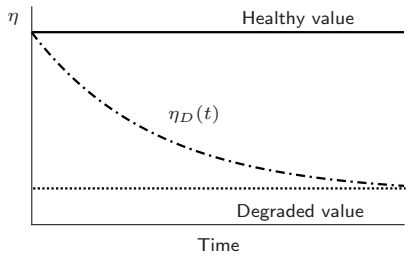

Fig. 1. Compressor efficiency as a function of time. If there is no degradation, healthy value of η is constant (solid black line). If the compressor degrades, then after a certain time η attains a new, degraded value (black dotted line). The transient $\eta_D \neq$ const (dash-dotted black line)

purposes in Section 4. Finally, conclusions and directions for future research complete the paper.

2. TURBOMACHINERY DEGRADATION

The degradation of rotating equipment, such as centrifugal compressors or turbines, is usually associated with fouling (Tarabrin et al., 1996). During steady-state operation, degradation can be measured by the deviation of the process variables from the expected, healthy values as described, e.g., by Loboda et al. (2007):

$$d = \frac{Y - Y_D}{Y} \tag{1}$$

where Y denotes the healthy value, and Y_D is the value in degraded state.

Usually, the undegraded value Y is delivered by the manufacturer of the compressor, whereas Y_D is estimated from thermodynamic relationships (Cicciotti, 2015) and shows the actual performance of the system. The ability to predict the value of Y_D would provide an insight into the future behaviour of the system. It could be estimated from (1), if the degradation indicator d was known, as:

$$Y_D = (1 - d) \cdot Y \tag{2}$$

Therefore, the question of modelling and predicting the degradation indicator d is considered, as it would provide knowledge on the degraded state of the system. It is usually assumed that the degradation is a function of only time in operation, $d = d(t)$ (Tarabrin et al. (1996), Jasmani et al. (2013)). This approach is justified in compressors working at the same operating point for the whole period.

Typically, the variables used for the degradation of turbomachinery are the head or the efficiency (Tarabrin et al., 1996). Figure 1 shows the behaviour of a compressor efficiency, $Y = \eta$, going from the healthy value η (solid line) to a certain degraded value (dotted line), usually after up to 2000 hours of operation (Tarabrin et al., 1996). The transient curve (dash-dotted line) shows the efficiency η_D as a function of time, $\eta_D(t) = (1 - d(t)) \cdot \eta$.

2.1 Degradation modelling

One of the possible approaches to predict the behaviour of the degradation indicator is based on trend analysis. The efficiency η_D of the degraded compressor is assumed to be a strictly monotonic, bounded function of time (decreasing), as depicted in Fig. 1. In consequence, the degradation indicator d calculated according to Eq. (1) would also be a strictly monotonic (increasing), function of time stabilising at a certain level.

Such behaviour suggests using an exponential function of time for approximation of $d(t)$, e.g. in form described by Tarabrin et al. (1996):

$$f(t, \beta) = \beta_1 - \beta_2 \exp(-\beta_3 (t - T_0)) \tag{3}$$

where t denotes time, and T_0 is the beginning of the degradation. It is usually assumed that T_0 is known, but not necessarily that $T_0 = 0$ (Cicciotti, 2015). Then $\beta = [\beta_i]$, $i = 1, \ldots, 3$ is a vector of constant parameters.

2.2 Degradation approximation

Exponential trend analysis was used, e.g., for monitoring by Cicciotti (2015) or maintenance planning by Xenos et al. (2016). However, in some industrial cases, the degradation indicator can be not monotonic and its convexity might change. An example of such case is depicted in Fig. 2. Figure 2a shows the actual efficiency of a compressor (black curve) compared with the expected value of 84% (blue horizontal line). The corresponding efficiency degradation indicator was calculated according to Eq. (1) and is presented as a function of time (in weeks) in Fig. 2b (black curve). The red curve shows the approximating function determined with Eq. (3).

The efficiency degradation described in Cicciotti (2015) follows the assumptions about the monotonicity, convexity, and boundedness of the indicator. However, Fig. 2b shows an indicator that saturates at 0.012 starting in week two, but then increases to 0.025 in week eight. Moreover, starting in week nine, the monotonicity changes, and the indicator starts to decrease.

The red curve shows the approximating function of form (3), with $T_0 = 0$ and parameters β_i found by minimising the square of a norm of the residuals $\mathbf{r}$ multiplied by a vector of weights $\mathbf{w} = [w_k]$

$$\min_{\beta} \sum_{k=1}^{n} w_k r_k^2 \tag{4}$$

with

$$\mathbf{r} = [r_k] = [f(x_k, \beta) - y_k] \tag{5}$$

where (t_k, y_k) are the observed data points, and w_k denote the weights of the measurements, here $w_k = 1$. The value of t_k denotes time and y_k is the corresponding value of efficiency degradation indicator, n indicates the number of measurements.

The approximating curve in Fig. 2b deviates from the actual value of the degradation indicator, starting from week three. This suggests that an approximation using a function with fixed shape is not sufficient.

3. APPROXIMATION WITH MOVING WINDOW AND SHAPE ADAPTATION

This section presents a method of updating the parameters of (3) using a moving window. The minimisation problem (4) is solved repeatedly with the optimisation constraints adapted to the varying shape in each period.

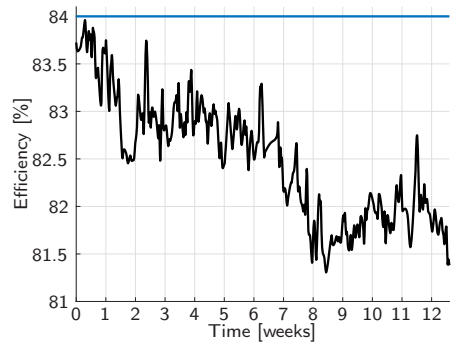

(a) Actual compressor efficiency (black line) and assumed efficiency if there was no degradation (blue line)

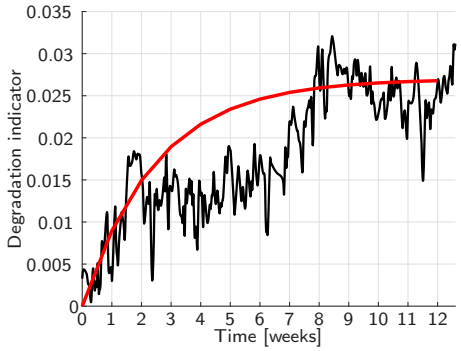

(b) Degradation indicator (black line) for data from Fig. 2a and approximating exponential function (red line)

Fig. 2. Example of compressor efficiency (Fig. 2a) and corresponding degradation indicator (Fig. 2b) from Brekke et al. (2009)

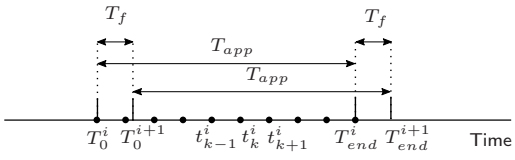

Fig. 3. Explanation of moving window notation

3.1 Moving window idea

The idea of a moving window approximation is depicted in Fig. 3. The ith approximation window starts at T_0^i, ends at T_{end}^i and has length T_{app}. The subsequent approximation window, $i+1$, is described with T_0^{i+1} and T_{end}^{i+1}, and has the same length, T_{app}. The time difference between two consecutive windows, $T_f = \Delta T_0 = \Delta T_{end}$, is also constant, and characterises the update rate of the approximation. The dots on the time axis denote the measurement instants t_k^i in ith window. In this work, $\Delta t_k = t_{k+1}^i - t_k^i = 1$ minute for all $t_k^i \in \left[T_0^i,\ T_{end}^i\right]$, for all i.

3.2 Approximation with shape adaptation

Rewriting Eq. (3) using the notation from section 3.1 yields:

$$f^i(t, \beta^i) = \beta_1^i - \beta_2^i \exp(-\beta_3^i (t - T_0^i)) \tag{6}$$

The parameter T_0^i denotes the start of the ith approximation window. The signs of β_2^i and β_3^i define the shape in the ith window, i.e. the monotonicity and convexity of the function, as indicated by the first and second time derivative, respectively (Davidson and Donsig, 2009). The parameter β_1^i shifts the approximating function up and down the vertical axis.

To allow adaptation to the varying shape of the degradation trend and in contrast to previous work where $\beta^{\mathbf{i}} > 0$, the constraints in the minimisation problem (4) are adjusted for the last element of the vector β^i, i.e. β_3^i. using the vector of differences $\mathbf{D}_i = \left[D_i^k\right]$ in the period $\left[T_0^i, T_{end}^i\right]$ calculated as

$$D_i^k = \frac{y_k - y_{k-1}}{t_k - t_{k-1}}\Big|_{t_k \in \left[T_0^i,\ T_{end}^i\right]} \tag{7}$$

Formula (8) applies a switching rule for β_3^i

$$\overline{\mathbf{D}}_i \begin{cases} \geq -0.0001, \text{then } \beta_3^i \in [0, \infty) \\ < -0.0001, \text{then } \beta_3^i \in (-\infty, 0] \end{cases} \tag{8}$$

where $\overline{\mathbf{D}}_i$ is the mean value of $\mathbf{D}_i$. The rest of the parameters are in the interval $[-3, 3]$. The values are found by consideration of typical rates of degradation and loss of performance of real machines.

The constraints for the parameter β^i allow the trend to follow the non-monotonic shape of the curves. The second issue is to force the system to follow the change in the trend of the indicator as soon as it happens, as the initial time is not known. This is done by adjusting the weighting vector, $\mathbf{w}$, to give less weight to older measurements in period $\left[T_0^i,\ T_{end}^i\right]$. Therefore, the weights are distributed in the interval $[0.9,\ 1]$ with the most recent measurements having the weights close to unity.

4. PREDICTION AND MONITORING

In this part, the algorithm using trend analysis is applied for monitoring of the degradation due to fouling and shown in Fig. 2. Two features of the algorithm are analysed: how accurate the prediction is, and how early the algorithm is able to predict a change in the trend of the indicator, depending on the parameters of the algorithm, T_{app} and T_f. The data come from a GE LM2500 engine operating offshore in the Norwegian Sea and were obtained from Brekke et al. (2009) using software developed by Rohatgi (2018). Accordingto Brekke et al. (2009), the data were collected during a period of operation without maintenance activities that could mitigate the loss of performance.

The idea of the prediction is depicted in Fig. 4. The function obtained after approximating the data in the interval $\left[T_0^i,\ T_{end}^i\right]$ (green lines) is extended into the next time period of length T_{pred} (blue lines). The end of the prediction window is marked with $T_{pred}^i = T_{end}^i + T_{pred}$. The arrows (red) show the differences between the actual values and the predicted curve.

4.1 Prediction accuracy

The differences between the actual values and the predicted curve are used for evaluating the accuracy of the

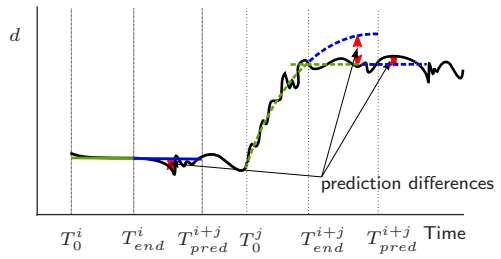

Fig. 4. Prediction idea with moving window approach

prediction for a given window, for instance of the ith window on the left side of Fig. 4. An indicator is proposed to evaluate the accuracy in ith window as:

$$SEP^i = \sum_{k=1}^{n} (y_k - f(t_k))^2 \tag{9}$$

where $t_k \in [T_{end}^i, T_{pred}^i]$. The higher the value of SEP^i, the further the prediction is from the actual data points, whereas $SEP^i = 0$ would mean that the prediction goes through each data point, capturing also the noise.

4.2 Prediction accuracy - results and discussion

The prediction results were evaluated as a function of T_{app}. Figure 5 shows how the mean value of SEP^i from Eq. (9) changes with the size of the approximating window (T_{app}) for a fixed value of the prediction window ($T_{pred} = 2$ weeks). An approximating window of less than 15 days resulted in high values of mean SEP^i, where 0.85 and above is considered high. If T_{app} is between 15 and 26 days, the mean SEP^i is below 0.8, and then increases again if $T_{app} > 26$. The quadratic approximation (orange line) in Fig. 5 suggests a robust minimum is at 20 to 21 days (three weeks). The explanation for this can be found by analysis of the black curve in Fig. 2b. It is visible that the two major changes of the trend of the degradation indicator last two weeks. They occurred in weeks one and two, and weeks eight and nine. Therefore, the approximation window of 21 days captures the entire transient behaviour and a short part of a neighbouring period. This allows the use of the properties of the approximating exponential function which follows this curvature.

To show the importance of T_{app}, two cases were chosen: $T_{app} = 14$ days (2 weeks), and $T_{app} = 21$ days (3 weeks). In both cases, shorter approximation period $T_{app} = 14$ days yielded larger value of mean SEP^i for two prediction periods, $T_{pred} = 14$ days and $T_{pred} = 4$ weeks. For $T_{pred} = 14$ days it was 0.8742 and 4.3072, whereas for $T_{pred} = 4$ weeks, it was 0.7661 and 3.455, respectively. The indicator was over four times higher when T_{pred} was longer. This suggests that trend analysis is better at short term predictions. It is confirmed by visual analysis of Fig. 2b. To accurately predict the efficiency degradation four weeks in the future, the trend would have to be constant for at least the summed lengths of the approximation and prediction windows, i.e. six weeks in this case. As there is no such period in Fig. 2b, the one month prediction is considered too long.

These results are also confirmed by the inspection of the efficiency indicators in Fig. 6 which presents the degradation indicator (black) and the approximating curves (red) for $T_{app} \in \{14, 21\}$ days, and $T_{pred} = 14$ days. The case $T_{pred} = 4$ weeks can be obtained directly by extrapolating the red curves and was omitted due to a space requirements. The period of two weeks is short enough to be contained almost entirely in a period with constant trend which results in incorrect predictions (Fig. 6a). Longer T_{app} captures the curvature of the indicator and the approximation follows the exponential trend (Fig. 6b) and is therefore chosen for further analysis.

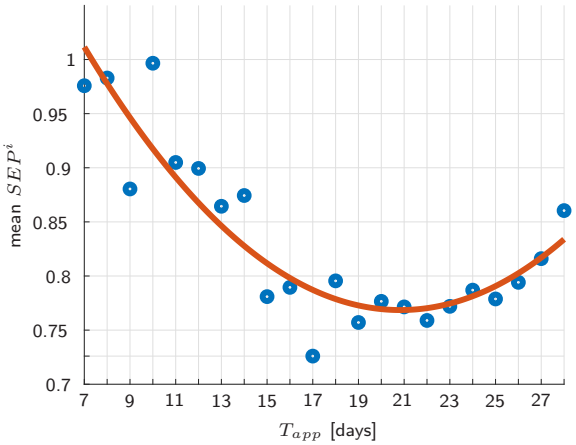

Fig. 5. The mean value of SEP as a function of T_{app}, for $T_{pred} = 2$ weeks and $T_f = 2$ days (blue points), with approximating quadratic function (orange line)

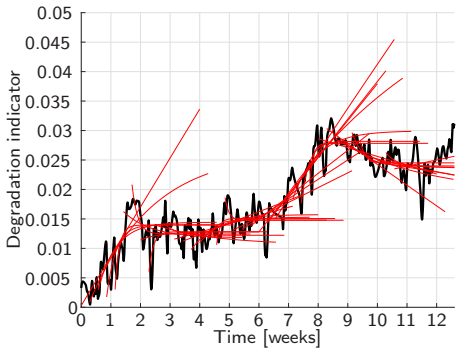

(a) $T_{app} = 2$ weeks

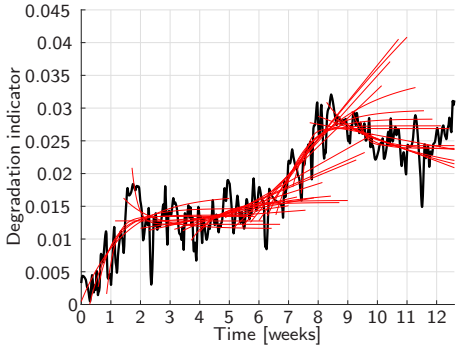

(b) $T_{app} = 3$ weeks

Fig. 6. Degradation indicator for $T_{pred} = 2$ weeks and T_{app} two and three weeks (solid black lines). The trend approximation and prediction are depicted in red

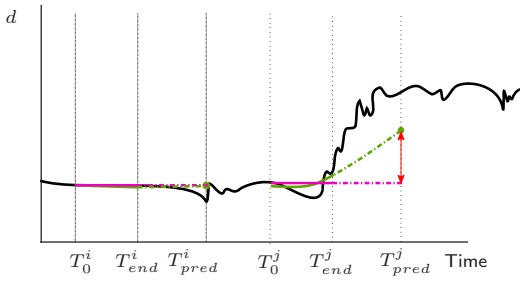

Fig. 7. The idea of using trend approximation for monitoring

4.3 Monitoring

In this section, the properties of the method from the point of view of monitoring are considered, i.e. if the algorithm were used on-line, how early the operator would get a prediction indicating future change in the trend of the degradation indicator. The idea of the detection algorithm has been depicted in Fig. 7. The black curve shows the values of the data, approximated with exponential trend (solid green curves) given by Eq. (6), then extrapolated in the prediction period (dashed green lines). The green dots denote the values of the trend approximation at the end of the prediction period. In addition, the pink lines denote the mean value of the real data in approximation window (solid lines). For the purpose of the evaluation, a change has been defined using the difference h^i (red arrows) between the final value of the approximating trend (green dot) and the mean extended in the prediction period (dashed pink lines):

$$h^i = f^i\left(T_{pred}^i, \beta^i\right) - \frac{1}{n}\sum_{k=1}^{n} y_k \tag{10}$$

where the parameters of $f^i\left(T_{pred}^i, \beta^i\right)$ are given by Eq. (6), with β^i found solving Eq. (4), and T_{pred}^i denoting the end of the ith prediction window. The corresponding approximation window contains n values of the degradation indicator, y_k, $k = 1, \ldots, n$. The absolute value of the difference h^i is compared with a predefined threshold θ. The change is detected if $|h^i| > \theta$.

The choice of θ depends on the operator. In this work, a change of 0.5 percentage points of efficiency is detected, i.e. $\eta - \eta_D = 0.5\%$. Taking $\eta = 84\%$ and using Eq. (1), the threshold θ is set to 0.006 in the degradation indicator.

4.4 Monitoring results and discussion

The detection algorithm was applied to data from Brekke et al. (2009). Figure 10 shows the data used for the analysis (black curve) obtained by removing the first two weeks from Fig. 2b to start from a steady state of the degradation process. The influence of the update rate, T_f, on the detection of an increasing trend in weeks eight and nine is analysed. The value of T_f is sought that would allow the earliest prediction. At the same time, T_f represents how often the approximation is performed, so to minimise the number of calculations, the largest possible T_f should be chosen. Then an application for online monitoring with selected parameters is presented. The prediction window

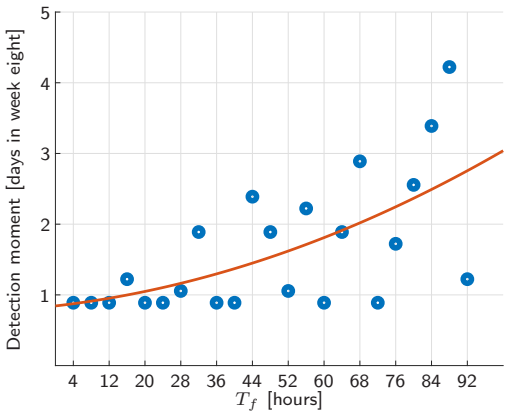

Fig. 8. The moment of detection as a function of T_f (blue points) and approximating quadratic curve (orange line)

was set $T_{pred} = 2$ weeks, i.e. the algorithm is set to detect a change in the next two weeks. The parameter T_{app} was set to 21 days (3 weeks).

Figure 8 presents the moment when the increase of the trend has been detected as a function of T_f. The horizontal axis shows the value of T_f, and the vertical axis shows the detection moment as day in week eight (blue points). The results were then approximated with a quadratic function (orange line), to emphasize the increasing value of T_{end}^i. Smaller values of T_f, below 44 hours, allow prediction earlier in week eight, at the expense of more frequent calculations. Larger T_f results in detecting the values up to three or four days later (T_f above 84 hours). Therefore T_f is chosen as 40 hours, as this allowed detection during the first two days of the week.

Figure 9 presents the evolution of the differences h^i as a function of time, with $T_{app} = 21$ days, $T_{pred} = 14$ days, $T_f = 40$ hours, and the threshold of 0.006. Two changes were detected – one in week eight, and one at the beginning of week twelve. The moments of detection have been marked with red dots. The approximation windows corresponding to the detected changes (also indicated with red dots) are depicted in Fig. 10, T_0^i, T_0^j – dotted lines, T_{end}^i, T_{end}^j – dash-dotted lines, $i < j$. The green curves show the approximating function, and pink horizontal lines show the mean values in the approximated periods. The corresponding differences h are marked with arrows, upwards if $h > 0$, downwards if $h < 0$.

The analysis of Fig. 9 provides an insight into the duration of the change detected in week eight. The values $|h^i|$ above the threshold show that the prediction is different than the mean, i.e. the trend in the corresponding approximating window is not constant. Increasing $|h^i|$ indicates the period where the prediction moves away from the actual value. However, decreasing value of $|h^i|$ indicates that the trend follows the curvature of the indicator and the prediction is getting closer to the mean, with the maximum of h^i indicating the transition. This implies that the change from week eight lasted two weeks, which is consistent with a visual analysis of Fig. 2, and thus confirms that the trend analysis might be used for monitoring.

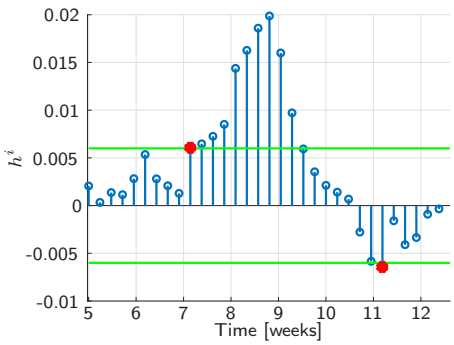

Fig. 9. The evolution of the change indicator h^i as a function of time (blue circles), with detection moments (red dots) and the threshold $\pm\theta$ (green horizontal lines)

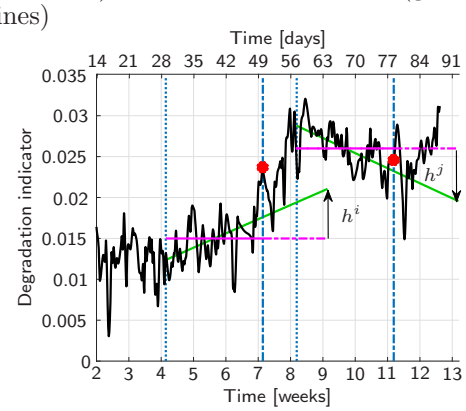

Fig. 10. The results of the monitoring with $T_{app} = 21$ days, $T_{pred} = 14$ days, $T_f = 40$ hours

The behaviour of h^i could also be used for decision support regarding the degradation. Positive and increasing h^i (detected in week eight in Fig. 9) means that the predicted value is larger than the mean in the ith window, and this suggests that the degradation would increase over the next prediction period. Negative value of h^i, on the other hand, shows a decreasing indicator (detected in week 12 in Fig. 9 and confirmed by a decreasing trend in Fig. 10). This suggests that the degradation would decrease and the performance might improve in the next prediction period.

5. CONCLUSION

Degradation monitoring is used with turbomachinery for purposes such as maintenance planning. Existing models of degradation assume that the degradation is strictly increasing with fixed convexity and that there are no additional changes during the considered operating period. Such behaviour is observed in certain industrial cases (Cicciotti, 2015), however, the shape of the degradation might change because of maintenance activities (Madsen and Bakken, 2014) or unexpected disturbances (Li and Nilkitsaranont, 2009). This work uses an exponential trend analysis with shape adaptation and applies it in a moving window framework to find the approximating model. The suggested adaptation method makes it possible for the model to follow the curvature of the degradation indicator.

The method is applied to the analysis of the evolution of the trend of the degradation. Two features of the algorithm are evaluated: the accuracy of the prediction depending on the length of the approximation window, and the capability of early detection of the change of the trend as a function of the update rate. The influence of the tuning parameters is investigated and recommendations for the values evaluated in a monitoring framework. Further work includes increasing the robustness over a variety of datasets and comparison with other monitoring approaches.

ACKNOWLEDGEMENTS

The authors would like to thank Dr James Ottewill from ABB Corporate Research Center in Poland for stimulating discussions and guidance.

REFERENCES

Brekke, O., Bakken, L.E., and Syverud, E. (2009). Compressor fouling in gas turbines offshore: Composition and sources from site data. In *ASME Turbo Expo 2009: Power for Land, Sea, and Air*, 381–391.

Cicciotti, M. (2015). *Adaptive Monitoring of Health-state and Performance of Industrial Centrifugal Compressors*. Ph.D. thesis. Imperial College London.

Davidson, K.R. and Donsig, A.P. (2009). *Real Analysis and Applications: Theory in Practice*. Springer Science & Business Media.

Hanachi, H., Mechefske, C., Liu, J., Banerjee, A., and Chen, Y. (2017). Enhancement of prognostic models for short-term degradation of gas turbines. In *2017 IEEE International Conference on Prognostics and Health Management*, 66–69.

Jasmani, M.S., Van Hardeveld, T., and Bin Mohamed, M.F. (2013). Performance degradation monitoring of centrifugal compressors using deviation analysis. In *Proceedings Of The 9th International Pipeline Conference*, 543–551.

Li, Y.G. and Nilkitsaranont, P. (2009). Gas turbine performance prognostic for condition-based maintenance. *Applied Energy*, 86(10), 2152–2161.

Loboda, I., Yepifanov, S., and Feldshteyn, Y. (2007). A generalized fault classification for gas turbine diagnostics at steady states and transients. *Journal of Engineering for Gas Turbines and Power – Transactions of the ASME*, 129(4), 977–985.

Madsen, S. and Bakken, L.E. (2014). Gas turbine operation offshore: On-line compressor wash operational experience. In *ASME Turbo Expo 2014: Turbine Technical Conference and Exposition*, V03BT25A008–V03BT25A008.

Rohatgi, A. (2018). Webplotdigitizer. URL `https://automeris.io/WebPlotDigitizer`.

Salamat, R. (2012). *Gas Path Diagnostics for Compressors*. Ph.D. thesis. Cranfield University.

Tarabrin, A.P., Schurovsky, V.A., Bodrov, A.I., and Stalder, J.P. (1996). An analysis of axial compressors fouling and a cleaning method of their blading. In *ASME 1996 International Gas Turbine and Aeroengine Congress and Exhibition*.

Xenos, D.P., Kopanos, G.M., Cicciotti, M., and Thornhill, N.F. (2016). Operational optimization of networks of compressors considering condition-based maintenance. *Computers & Chemical Engineering*, 84, 117–131.